ADVANCED MATERIALS INTERFACES
www.advmatinterfaces.de

Recent Advances in Large-Scale Tactile Sensor Arrays Based on a Transistor Matrix

Zhihao Huo, Yiyao Peng, Yufei Zhang, Guoyun Gao, Bensong Wan, Wenqiang Wu, Zheng Yang, Xiandi Wang, and Caofeng Pan**

Tactile sensors that possess the physical properties of human epidermis, which can sense external stimuli (pressure, temperature, humidity, etc.), are a very popular cutting-edge innovation. They make a large contribution to extensive applications in the real-time monitoring of human health, artificial intelligence, robot systems, and biocompatibility. However, great challenges remain in large-scale tactile simulation to attain fast data transmission and low signal crosstalk among the pixels. The tactile sensor arrays based on a transistor matrix (TSATMs) are thus investigated for large-scale pressure mapping. Currently, a variety of TSATMs with different device structures have been described. The integrated composite structure, consisting of a transistor matrix and a pressure-dependent electronic component, was first widely employed for tactile mapping. Then, researchers conducted a large amount of scientific inquiry into the intrinsic pressure-sensitive transistor. These pressure-dependent transistors are based on changes in the specific gate capacitance, piezotronic effect, piezo-phototronic effect, and triboelectric nanogenerator. Certainly, novel systems and materials, low-power consumption, and multifunctional design should be considered for the next generation of intelligent TSATMs to meet the needs of diverse practical applications.

1. Introduction

Tactile sensing refers to the way that humans obtain external environmental information by touching objects.[1] Indeed, humans interact with nature through the skin, which is the largest tactile receptor. Researchers have explored various tactile sensors that can imitate multiple environmental stimuli, such as touch, stress, strain, humidity, and temperature, via electronic methods. In recent years, the development of tactile sensors has become a cross-disciplinary field that integrates a wide range of expertise in electronics, physics, materials science, chemistry, and biology.[2] At the same time, significant breakthroughs in flexible electronics, nanotechnology, and manufacturing have enabled the construction of tactile sensors with superior performance based on different transduction methods, including piezoresistivity,[3] capacitance,[4] and piezoelectricity.[5] More specifically, large-scale skin-like tactile sensors that detect pressure, temperature, or other stimuli in the surroundings have attracted increasing attention for applications in human–machine interfaces,[6] intelligent robots,[7] artificial limbs,[8] and other intelligent systems.[9] However, certain challenges remain in large-scale tactile simulation with fast data transmission and low signal crosstalk among the pixels.

The tactile sensor arrays based on a transistor matrix (TSATM) have thus been developed for large-scale 2D tactile profiles.[10] The field effect transistor (FET) is one of the most important components in every electronic device, and it has three lead-out electrodes, the source, drain, and gate electrodes. It can control the flow of electrons through a planar channel when the applied gate voltage exceeds a certain threshold. In this way, small changes in the input voltage can excite the transition between high and low output currents. Thus, the FET operates as a control device and amplifier in a logic circuit.[11] A transistor active matrix is necessary to be employed in a large-scale tactile sensor, where the addressing mode is similar to the memory structure, with word lines and bit lines. Large-scale tactile mapping can be easily achieved by monitoring the drain/source current of each pixel. At the same time, the one-way current-passing characteristics of the transistor make it possible to reduce the crosstalk among the pixels. Recently, various types of TSATMs with outstanding performance based on an integrated composite structure or intrinsic pressure sensitive transistor were consecutively demonstrated for a variety of actual applications, as shown in **Figure 1**.

This review focuses on the introduction of advanced TSATMs. The main content includes the following aspects: i) various types of TSATMs with an integrated composite structure that consists of a transistor matrix and a pressure-dependent electronic component, and the development of the

Z. Huo, Y. Peng, Y. Zhang, G. Gao, B. Wan, W. Wu, Z. Yang, Prof. X. Wang, Prof. C. F. Pan
CAS Center for Excellence in Nanoscience
Beijing Key Laboratory of Micro-nano Energy and Sensor
Beijing Institute of Nanoenergy and Nanosystems
Chinese Academy of Sciences
Beijing 100083, P. R. China
E-mail: wangxiandi@binn.cas.cn; cfpan@binn.cas.cn
Z. Huo, Y. Peng, G. Gao, Z. Yang, Prof. X. Wang, Prof. C. F. Pan
School of Nanoscience and Technology
University of Chinese Academy of Sciences
Beijing 100049, P. R. China
The ORCID identification number(s) for the author(s) of this article can be found under https://doi.org/10.1002/admi.201801061.

DOI: 10.1002/admi.201801061

TSATM for different applications has also been indicated; ii) intrinsic pressure-sensitive transistors based on the change in the specific gate capacitance of the transistor, and iii) intrinsic pressure-sensitive transistors based on piezotronic effect,[12] piezo-phototronic effect,[13] and triboelectric nanogenerator (TENG).[14] The piezoelectric potential or triboelectric potential can act as the gate voltage. In the end, we introduce some extraordinary representatives and innovative work on TSATMs, and we summarize the existing challenges and novel trends for the next generation of the TSATM.

2. Basic Concepts for the Field Effect Transistor

2.1. FET Structure and Classification

FETs can be classified into n-channel devices and p-channel devices according to the types of channel carriers (**Figure 2**a,b).[15] For the n-channel devices, the conductivity increases with the enhancement of the positive gate voltage because their carriers are electrons. In contrast, the conductivity of the p-channel devices shows a positive correlation with the negative gate voltage due to their hole carriers. Notably, it is important to describe the state of the transistor at zero gate voltage.[16] If the channel conductance is very low at zero gate voltage, a positive voltage must be applied on the gate to form the n-channel, and then, the device is an enhancement (normally off) n-channel metal-oxide-semiconductor field effect transistor (MOSFET). If n-channel exists at zero gate voltage, a negative gate voltage must be applied to deplete the carriers in the channel to reduce the channel conductance. This type of device is a depletion (normally on) n-channel MOSFET. Accordingly, an enhancement n-channel device will possess a drain current significantly only if a positive V_{GS} (gate voltage) greater than V_T (threshold voltage) is applied. For a depletion n-channel device, a large current flows when $V_{GS} = 0$, and thus, the current can be increased or decreased by changing the gate voltage. Similarly, p-channel enhancement and depletion MOSFETs share the same principle (Figure 2b).[17]

2.2. Physical Characteristics of the Transistor

The physical characteristics of an MOSFET can be explained by discussing its output characteristics and transfer characteristics. Figure 2c shows the ideal source–drain characteristic of the MOSFET. The dashed line separates the curves into three regions, including linear, nonlinear, and saturation zones. Assuming a situation where a voltage is applied on the gate to form an inversion layer in the semiconductor surface, current flows from the source to the drain through the channel when a small drain voltage (V_{DS}) is applied. In this case, the channel works as a resistor, and the drain/source current (I_D) is proportional to V_{DS}, which responds to a linear region. Then, the current deviates from a linear relationship with an increase in V_{DS} because the charge near the drain has been reduced by the channel potential until it reaches a point (pinch-off point) where the inverting layer charge at the drain is almost zero. Eventually, the I_D is maintained at an essentially constant value (saturation region) while the V_{DS} continues to increase. Spontaneously, three regions of the MOSFET output characteristic curve correspond to different current equations. Specifically, the current equation at the linear region has a significant potential role for designing and improving the transistors that are used in tactile sensors, as follows

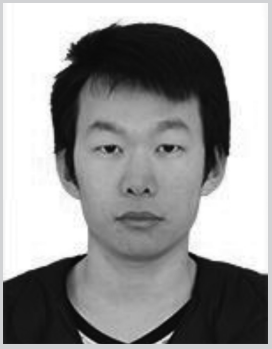

Zhihao Huo received his undergraduate degree from the University of Jinan in 2016. Currently he is pursuing his PhD under the supervision of Prof. Caofeng Pan at Beijing Institute of Nanoenergy and Nanosystems, Chinese Academy of Sciences. His current research interests focus on low-dimensional piezoelectric semiconductor micro/nanophotoelectric function device.

Xiandi Wang received his PhD degree in condensed matter physics from the University of Chinese Academy of Sciences in 2016. He had been a postdoc fellow in the group of Professor Zhong Lin Wang at National Center for Nanoscience and Technology. Now he is an associate professor in the group of Prof. Caofeng Pan at Beijing Institute of Nanoenergy and Nanosystems, CAS since 2018. His research interests mainly focus on the fields of piezo-photonic effect and triboelectric nanogenerator for fabricating novel flexible large-scale tactile sensor matrix and stretchable electronics.

Caofeng Pan received his BS degree (2005) and his PhD (2010) in materials science and engineering from Tsinghua University, China. Then he joined the group of Professor Zhong Lin Wang at the Georgia Institute of Technology as a postdoctoral fellow. He is currently a professor and a group leader at Beijing Institute of Nanoenergy and Nanosystems, Chinese Academy of Sciences since 2013. His research interests mainly focus on the fields of piezotronics/piezo-phototronics for fabricating new electronic and optoelectronic devices, tactile sensors and self-powered nanosystems. Details can be found at http://www.piezotronics.cn/.

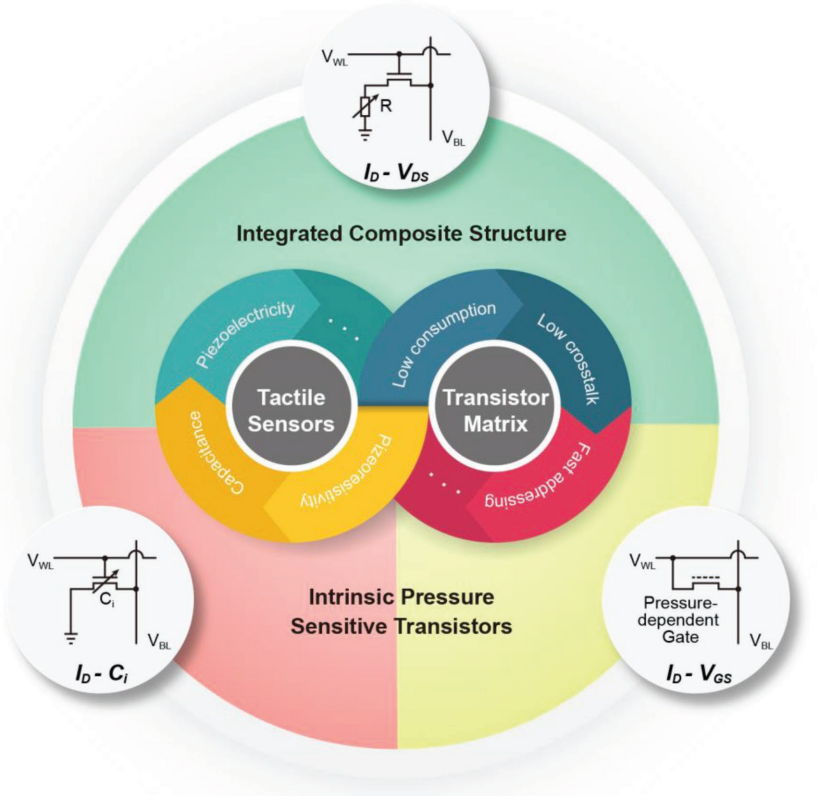

Figure 1. Various types of TSATMs. Different tactile sensors were demonstrated based on the piezoresistivity, capacitance, and piezoelectricity. For large-scale tactile mapping, the transistor matrix was employed with low power consumption, low crosstalk, and fast addressing. The integrated composite structure and the intrinsic pressure sensitive transistors were widely used in TSATMs. The insets show the circuit diagram of each pixel in different types of TSATMs.

$$I_D = \frac{W}{L} \cdot \mu \cdot C_i \cdot (V_{GS} - V_T) \cdot V_{DS} \quad (1)$$

where V_{DS} and I_D are the drain/source voltage and current, respectively, V_{GS} and V_T represent the gate voltage and threshold voltage, respectively, C_i is the specific gate capacitance, μ is the mobility, and L and W stand for the channel length and width, respectively. The extrapolated value on the V_{GS} axis is equal to V_T +1/2 V_{DS}, and the deviation from linearity at a higher V_{GS} value is attributed to the decrease in mobility.

3. Tactile Sensor Arrays Based on the Transistor Matrix

The large-scale tactile sensor is one of the most important trends in the field of wearable devices for the ability to simulate the human touch sense over a large area, and it is related to the development of next-generation intelligent and multifunctional electronic devices.[18] The key challenges for large-scale tactile sensor arrays are how to optimize the device structure for data transmission of a large number of pixels and how to minimize the signal crosstalk among the pixels. Therefore, the TSATM was developed to realize the 2D large-scale pressure mapping.[19] Similar to the memory structure, the number of addressing lines was drastically reduced to m + n for an m × n sensor array by using the addressing mode with word lines and bit lines, which results in the simplification of a structure. On the other hand, the one-way current-passing characteristic of the transistor makes it possible to reduce the crosstalk among the pixels and complete the tactile mapping with low power consumption at the same time. Recently, significant breakthroughs have been achieved on large-scale and flexible TSATMs based on different transduction methods that convert mechanical stimuli into electronic signals, including piezoresistivity, capacitance, and piezoelectricity.[20] An overview of various methodologies, materials, and technologies for the development of transistor switch performances, including the pressure sensitivity of tactile sensors and the optimal design method of device structures, will be presented in this section.

3.1. Basic Device Structure of the TSATM

By assembling a transistor matrix to be used as an electronic switch with a pressure-dependent electronic component, as

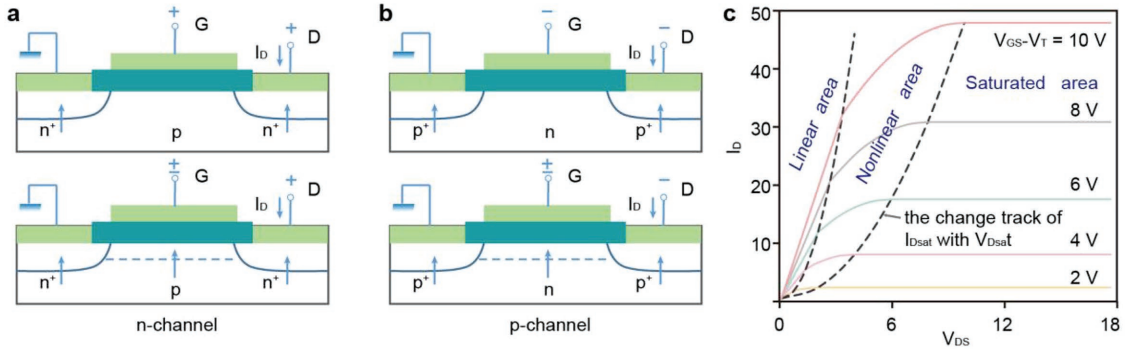

Figure 2. Schematic diagrams of the FET structure and physical characteristics. a) Enhancement n-channel FET and depletion n-channel FET. b) Enhancement p-channel FET and depletion p-channel FET. c) Drain characteristics of an ideal FET.

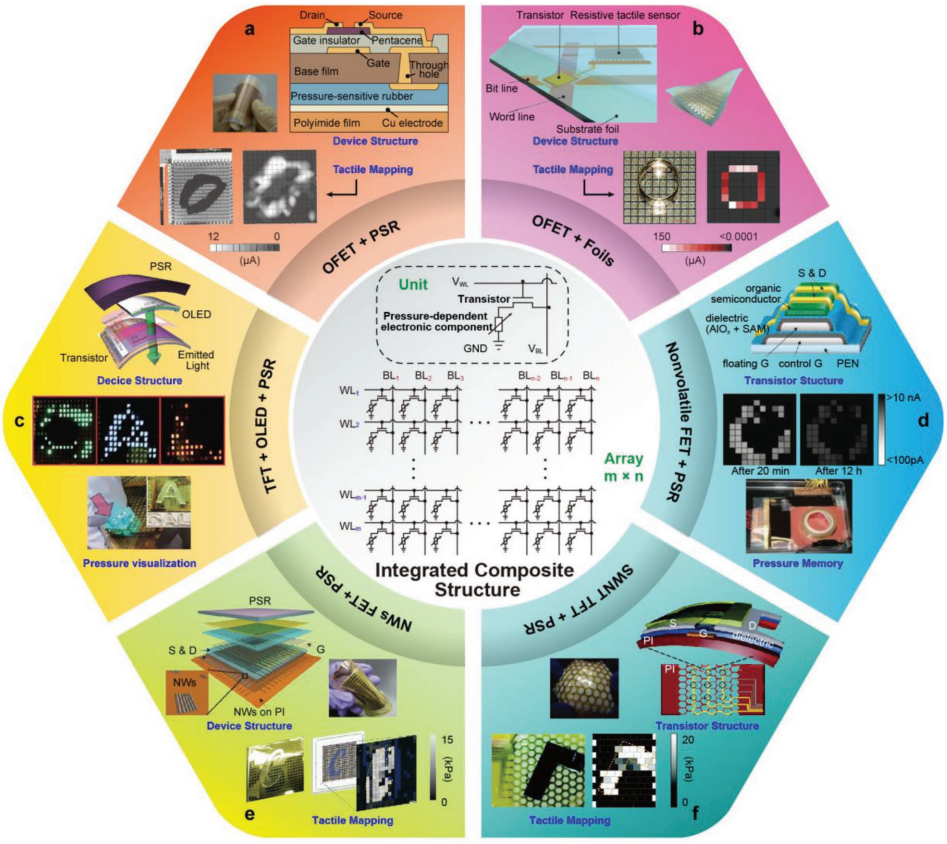

Figure 3. Different TSATMs based on the integrated composite structure. Middle: Circuit diagrams of the TSATM and each unit. Each pixel consists of a transistor and a pressure-dependent electronic component. a) OFET + PSR: OFET active matrix integrated with a pressure-sensitive rubber layer for tactile mapping. Reproduced with permission.[21] Copyright 2004, National Academy of Sciences. b) OFET + Foils: OFET arrays integrated with ultrathin polymer foils. Reproduced with permission.[23] Copyright 2013, Macmillan Publishers Ltd. c) TFT + OLED + PSR: Carbon nanotube TFTs integrated with a PSR layer and OLEDs for pressure visualization. Reproduced with permission.[24] Copyright 2013, Macmillan Publishers Ltd. d) Nonvolatile FET + PSR: A nonvolatile memory organic floating-gate transistor matrix integrated with a PSR layer to store the pressure spatial distribution. Reproduced with permission.[25] Copyright 2009, American Association for the Advancement of Science. e) NWs FET + PSR: TSATM based on the parallel oriented Ge/Si nanowire arrays with higher carrier mobility. Reproduced with permission.[27] Copyright 2010, Macmillan Publishers Ltd. f) SWNT TFT + PSR: TSATM based on the SWNTs with an excellent on/off current ratio. Reproduced with permission.[29] Copyright 2011, American Chemical Society.

shown in the middle of **Figure 3**, TSATMs can be employed to map the strain distribution over a large area, which is an approach that has attracted a large amount of attention for applications in artificially intelligent e-skin. In 2004, Someya et al. first used this structure of the TSATM, which consisted of an organic field-effect transistor (OFET) active matrix and a pressure-sensitive rubber (PSR) layer, to obtain a satisfactory tactile profile, as shown in Figure 3a.[21] A flexible 16 × 16 pixelated TSATM was demonstrated with a resolution of 10 dpi. The gate/drain electrodes, the word/bit lines, served as the addressing lines of the switching matrix. The pressure-dependent PSR layer as variable resistance was integrated between the source electrode and the ground. The transistor worked by providing a high voltage on the corresponding word line and bit line; in other words, it could turn a single pixel circuit on while others were in a closed state. Upon strain, the resistance of the PSR changes, which leads to variation in the source–drain current in a pixel unit. Thus, a 2D pressure distribution could be easily achieved by monitoring the current of each pixel. In other words, the pressure-dependent electronic component in the basic device structure of the TSATM presents the pressure information of each pixel, and the transistor stitching matrix provides a chance to obtain a large-scale tactile mapping with low signal crosstalk and power consumption.

Until now, different types of TSATMs based on this integrated composite structure were further exploited for higher performance or various practical applications. On the one hand, different pressure-dependent source–drain resistance was designed into the pixel circuit. At first, the PSR layer, a type of conductive polymer composite, was widely used in the TSATM. Conductive fillers, such as carbon black and carbon fiber, are added into an elastomeric polymer to form the polymer composites used to achieve the outstanding conductivity and mechanical properties.[22] Recently, an ultrathin polymer foil was used as the pressure-dependent electronic component instead of the PSR layer, as shown in Figure 3b.[23] The surface conductivity changed when other objects connected to the foil. The utilization of foils can further enhance the resolution of tactile sensors with low signal interference among pixels and ensure the device to be thinner and lighter with

excellent performance at the same time. Additionally, the sensor can withstand repeated bending with a radius of 5 μm and can work under a high temperature or water environment, and thus, it is expected to be applied in mobile electronic devices, sports, robotics, and biomedical systems. In addition, Javey's group demonstrated a user-interactive TSATM for pressure visualization.[24] Organic light emitting diodes (OLEDs) and PSR layers were coupled in series to serve as the source–drain resistance (Figure 3c). With an increase in the pressure, the conductivity of the PSR layer is enhanced due to the formation of a shorter conductive path, which caused these OLEDs to be lit. Hence, the visual luminescent intensity of the OLEDs in each pixel unit could respond to the partial pressure on the device. Moreover, it is worthwhile to mention that a high source–drain current was acquired by using the thin-film transistor based on the carbon nanotubes, which played a crucial role in driving OLED pixels. Additionally, it is possible to achieve a digital pressure mapping by monitoring the drain current. Moreover, Someya's group demonstrated a nonvolatile memory transistor by laminating a floating gate in the hybrid dielectrics of the organic transistor (Figure 3d).[25] By integrating it with the PSR layer, the TSATM could realize the storage of the 2D strain distribution for a long period due to having less charge loss in the floating gate. Thus, many novel TSATMs can be designed by optimizing the electronic components in the unit circuit for a variety of practical applications.

On the other hand, transistors play an important role in data transmission, with fast response time and fine image quality of the tactile mapping. Therefore, it is vital to use certain semiconductor materials to develop transistors with excellent switching characteristics, including carrier mobility, operating voltage, and on/off current ratio. Compared with the OFETs, which allow the TSATMs to be more flexible, transistors composed of inorganic semiconductors as active channel materials possess higher carrier mobility and lower operating voltage, as shown in Figure 3e.[26] Javey and co-workers successfully exhibited an 18 × 19 flexible TSATM based on the parallel oriented Ge/Si nanowire (NW) arrays.[27] The transistor matrix could operate at a low operating voltage of less than 5 V. Simultaneously, the device possessed fine mechanical robustness and remarkable electrical properties, which could also detect the pressure distribution after more than 2000 cycles, with a bending radius of 2.5 μm. In addition, single-walled carbon nanotubes (SWNTs) have been widely employed in the transistors due to the ability of extensibility, transparency, and solution-based processing.[28] Ali's group also demonstrated a high-performance TSATM based on the highly semiconductor-enriched (99%) SWNTs (Figure 3f).[29] The thin-film transistor (TFT) switching matrix exhibited a whole mobility of 20–30 $cm^2\ V^{-1}\ s^{-1}$ and excellent I_{ON}/I_{OFF} ($\approx 10^4$).

Notably, stretchable electronics have attracted increased attention as alternative future electronics for applications in human–machine interaction due to their excellent adhesion properties.[30] However, there remain great challenges in finding suitable materials and fabrication techniques to achieve a large-scale stretchable TSATM. Recently, researchers have focused on the fabrication of stretchable transistors and the integrated design of the device. Someya and co-workers dispersed SWNTs and ionic liquids (reusable and recyclable) equally into a fluorinated copolymer matrix to achieve a SWNT composite film that possessed an unusual electrical conductivity of 57 siemens per centimeter and a stretchability of 134%, as shown in **Figure 4**a.[31] By integrating the printed organic transistors, a 19 × 37 stretchable transistor matrix was successfully demonstrated, which also exhibited fine mechanical robustness and excellent electrical properties. Ha and co-workers developed a stretchable temperature sensor matrix based on the SWNTs TFT with polyaniline nanofibers, which could detect the temperature distribution.[32] Additionally, various materials were further investigated in Bao's group to enhance the stretchability of the transistor. By using microcracks of organic intrinsic semiconductors, a scalable organic transistor could be stretched up to a 250% strain.[33] They also exhibited self-healing organic semiconductors by adding modified side-chains and segmented backbones into flexible molecular building blocks.[34] The organic thin-film transistors (OTFTs) fabricated from these materials showed excellent electrical properties and admirable stretchability. Moreover, the investigators explored novel technologies and methods for stretchable electronics. In 2017, they described the nanoconfinement of polymers and made the synthesized polymer semiconducting film stretch up to a 100% strain with a high mobility of 1.32 $cm^2\ V^{-1}\ s^{-1}$[35] Then, a fully stretchable transistor was demonstrated, which consisted of the fabricated semiconducting film, carbon nanotube networks, and polystyrene-block-poly(ethylene-co-butylene)-polystyrene, as shown in Figure 4b. The TFT device exhibited excellent electrical properties and mechanical stability, with the mobility of 0.55 $cm^2\ V^{-1}\ s^{-1}$ under a 100% strain, while it also showed fine transparency and great conformability. For practical applications, they displayed a skin-like finger-wearable driver in which the transistor served as the light-emitting diode (LED) driver, and the LEDs could stably work regardless of how much the fingers bent or contracted. Furthermore, they developed a fully extensible TSATM that was based on intrinsically stretchable conductors (Figure 4c).[36] Such a sensor with stretchable integrated circuits for signal manipulation and computation could be easily mass-produced with an average of 347 transistors per square centimeter. These sensors accurately detected the footprint of a small ladybug through a matched map of on-current magnitudes. At the same time, the fabrication technology of the device provided a versatile processing platform for the incorporation of other intrinsically stretchable polymer materials. This approach would make it possible to manufacture next-generation stretchable electronic devices and commercialize them in the future.

3.2. Structure-Optimized TSATM with Pressure-Dependent Transistors

Miniaturization and integration are the two major factors for the manufacturing technology and engineering application of the TSATM. For this reason, researchers around the world continue a multipronged effort to develop the structure-optimized TSATM in which the electrical properties of the transistor are related to the pressure; in other words, the device did not require an extra pressure-dependent electronic component (**Figure 5**a).[37] As previously discussed, the drain/source current (I_D) depends on the dielectric capacitance (C_i) according

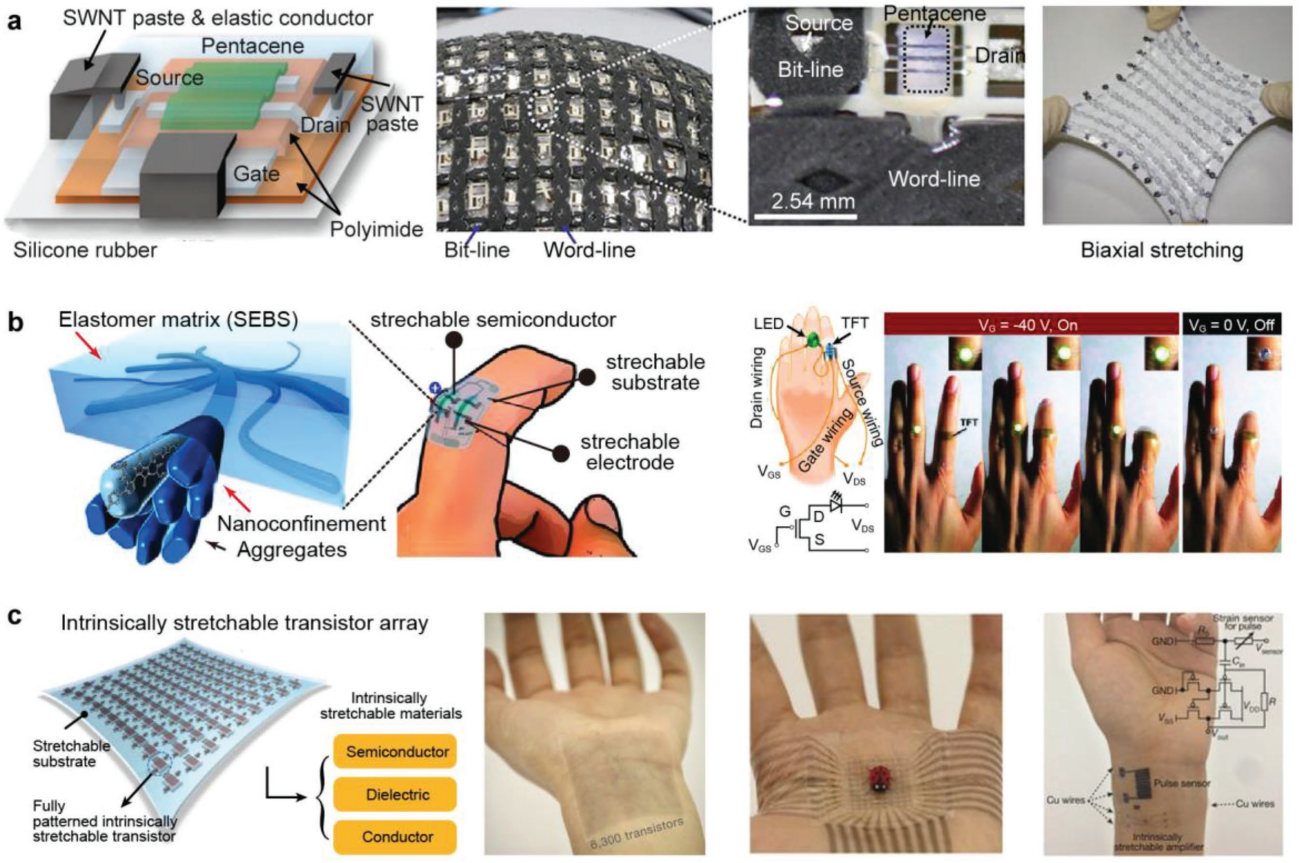

Figure 4. Stretchable TSATM. a) Large-area stretchable active matrix integrated with organic transistors and SWNT elastic conductor. Reproduced with permission.[31] Copyright 2008, American Association for the Advancement of Science. b) Transistor arrays based on the polymer semiconducting film with enhanced stretchability by nanoconfinement. Reproduced with permission.[35] Copyright 2017, American Association for the Advancement of Science. c) Intrinsically stretchable transistor arrays and circuits for tactile sensing. Reproduced with permission.[36] Copyright 2018, Macmillan Publishers Ltd.

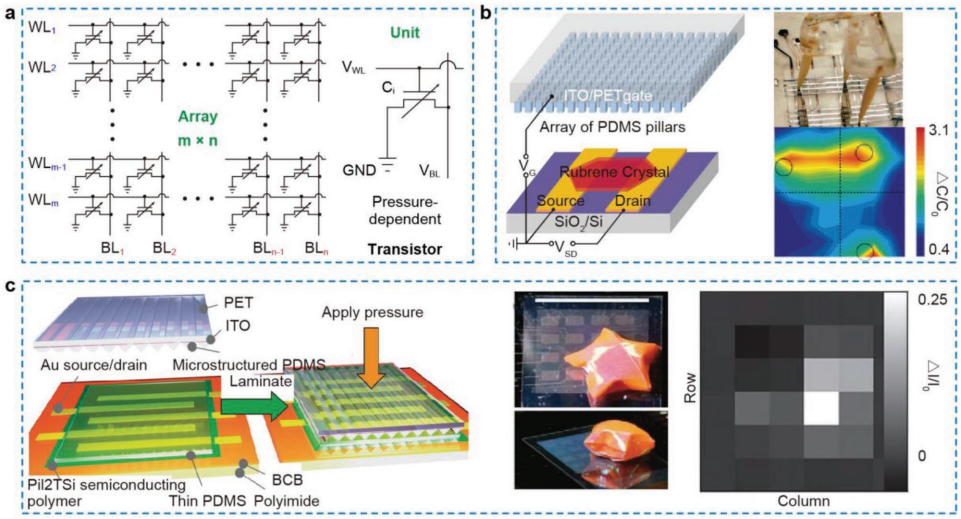

Figure 5. Intrinsic pressure-sensitive transistor based on changes in the specific gate capacitance. a) Circuit diagram of the TSATM based on the capacitance-dependent transistors. b) Pressure-dependent transistors with microstructured PDMS dielectric film. a,b) Reproduced with permission.[38] Copyright 2010, Macmillan Publishers Ltd. c) Large-scale flexible TSATM with the microstructured elastic dielectric for pressure mapping. Reproduced with permission.[40] Copyright 2013, Macmillan Publishers Ltd.

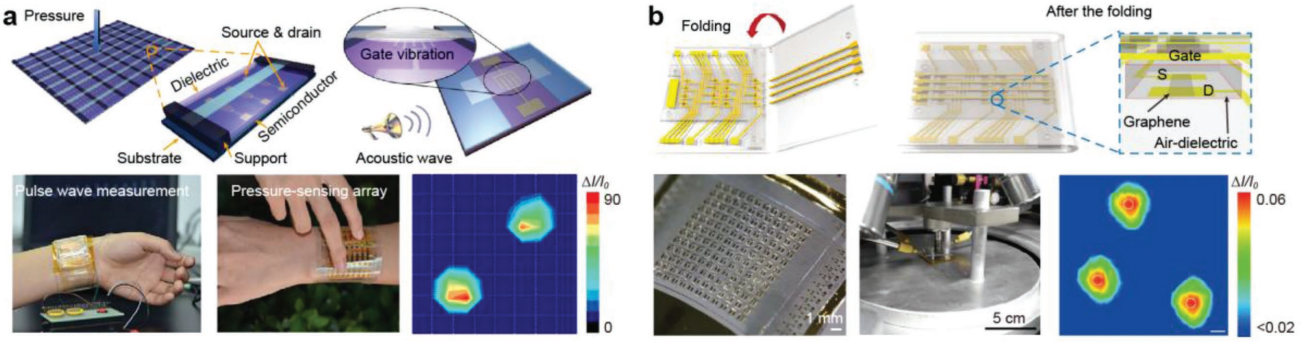

Figure 6. Various dielectric materials and novel structures for TSATMs. a) TSATM based on the suspended gate organic thin-film transistor for the detection of ultralow pressure. Reproduced with permission.[42] Copyright 2015, Macmillan Publishers Ltd. b) TSATM based on the novel transistor arrays for wide pressure ranges by using the folded structure. Reproduced with permission.[43] Copyright 2017, Macmillan Publishers Ltd.

to the formula (1). Instead of the rigid dielectric, the elastic dielectric will deform more or less when strain was applied, which leads to a change in the dielectric capacitance of the transistor. Consequently, the I_D of the transistor will change quickly when the device is under strain. Bao's group pioneered the use of microstructured compressible gate dielectrics to fabricate a highly sensitive pressure-dependent transistor, as shown in Figure 5b.[38] The utilization of the pyramid-structured polydimethylsiloxane (PDMS) made the dielectric more deformable, and thus, the transistor possessed better pressure sensitivity in the low-pressure regime (less than 2 kPa) due to the introduction of a larger air gap (a lower dielectric constant of ≈1.0 compared with PDMS (≈3.0)).[39] Furthermore, the investigators successfully demonstrated a large-scale flexible pressure-sensitive TSATM on the polyimide substrate for an application on the detection of static pressure and human health monitoring (Figure 5c).[40] The OTFT based on microstructured rubber possessed a pressure sensitivity of 8.4 kPa^{-1} and a fast response time of <10 ms. Obviously, this structure-optimized tactile sensor matrix based on the pressure-dependent transistors has more excellent pressure sensitivity compared with the TSATM based on the PSR. Therefore, these devices could accurately monitor weak pressure signals such as pulse waves in the human radial artery.

A variety of dielectric materials or novel structures were further investigated to obtain TSATMs with different pressure sensitivity, detection limits and measurement ranges. The utilization of an air gap has attracted growing interest as an alternative dielectric material in the transistor for the potential application of ultrahigh sensitive pressure detection. Recently, different types of capacitance-dependent tactile sensors with air gaps were demonstrated. Viry et al. proposed a three-axial pressure sensor based on a flexible floating fluorosilicone dielectric layer and a nonstretchable copper/tin coated electrode fabric.[41] It was worthwhile to note that an ≈150 µm air gap naturally formed between the two textile electrodes due to the low adhesion characteristics of fluorosilicone. The air gap acting as the second dielectric layer of the sensor made it possible to exhibit high sensitivity under an extremely low pressure condition. Moreover, Zang et al. developed a suspended gate organic thin-film transistor that employed an air dielectric layer and suspended gate electrodes to enhance the pressure sensitivity of the TSATM (**Figure 6**a).[42] This flexible pressure sensor possessed notably ultralow pressures of <0.5 Pa, ultrahigh pressure sensitivity (192 kPa^{-1}), and low power consumption (<100 nW) under an operating voltage of 6 V, which was sufficient to detect the human pulse and sound pressure. They also integrated OTFTs on a polyethylene terephthalate to fabricate a flexible 8 × 8 pixelated sensor arrays for spatial pressure mapping. On the other hand, some researchers have extensively studied the development of novel structure and manufacturing methods to expand the measurement range of the TSATM. Shin et al. introduced an unusual manufacturing method to produce pressure-sensitive graphene FET with novel dielectric layers (Figure 6b).[43] An air-dielectric layer would be formed by folding an origami substrate with the two opposing plastic panels and a foldable elastic joint. The graphene channels, source/drain electrodes, and elastic separation gasket of the PDMS were patterned on one panel, while the gate electrode was deposited on another panel. Compared with the transistors with floating gates, this design of an origami substrate brought a clean interface between the air dielectric layer and graphene, which not only reduced the hysteresis effect of the pressure sensors but also obtained a higher resolution and wider tactile pressure sensing range. The synthesized 50 × 50 TSATM could map the 2D pressure distribution with the wide pressure range of 250 Pa to 3 MPa, which had excellent potential applications in prosthetic devices and medical diagnosis.

3.3. Structure-Optimized TSATM without a Gate Electrode

The utilization of pressure-dependent transistors makes the structure of TSATMs simpler due to the omission of extra pressure-sensitive media. However, it is a large challenge for the manufacturing processes to use those elastic dielectrics in the transistor. Additionally, traditional FETs based on voltage-gated operations belong to three-terminal devices, which limits the resolution of the TSATM to a certain extent. Therefore, a new device structure should be designed to acquire a high-resolution tactile sensor. For a high-density functional nanodevice, it is an effective solution to omit the interconnect layout of the gate electrode, in other words, the TSATM changes from a three-terminal to a two-terminal device.[44] Wang's group has sustainably

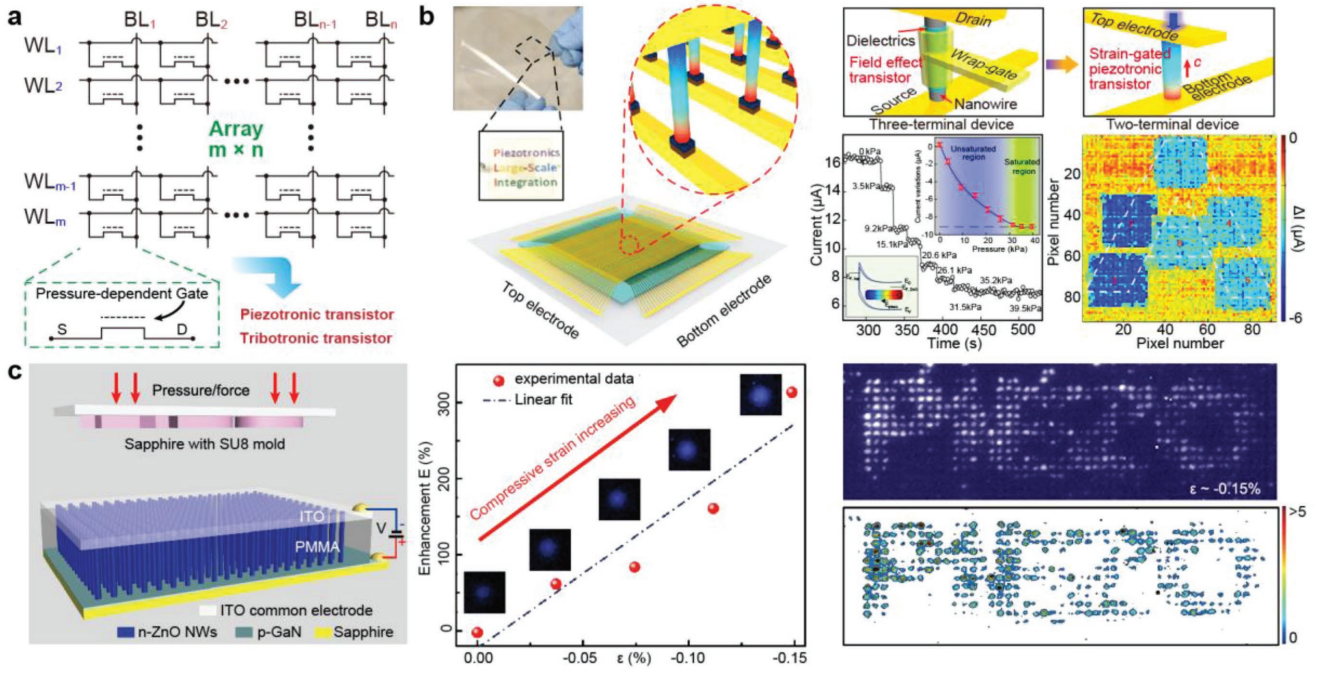

Figure 7. Intrinsic pressure-sensitive transistor based on the piezotronic effect and piezo-phototronic effect. a) Equivalent circuit diagram of structure-optimized TSATMs by using the piezopotential as the gate voltage. b) High-resolution TSATM with piezotronic transistors based on ZnO NWs arrays for pressure mapping. a,b) Reproduced with permission.[49] Copyright 2013, American Association for the Advancement of Science. c) Nanowire light-emitting diode pressure sensor arrays with a fast response time based on the piezo-phototronic effect. Reproduced with permission.[50] Copyright 2013, Macmillan Publishers Ltd.

developed a series of piezoelectric sensors based on piezotronic and piezo-phototronic effects by using piezoelectric semiconductor materials, including ZnO,[45] GaN,[46] and CdSe.[47] A piezopotential is induced in the crystal due to the noncentral symmetry under strain.[48] It has a significant influence on the control of the charge carrier transport properties at the interface/junction, which can be regarded as a "gate" voltage in a three-terminal device, as shown in **Figure 7**a. Hence, it offers the chance to reduce the number of electrodes for the fabrication of high-resolution TSATMs.

A high-resolution large-scale 92 × 92 TSATM that consists of ZnO NWs was based on the strain-gated piezoelectric transistor matrix, as shown in Figure 7b.[49] These piezoelectric transistors could directly convert external stimuli into electrical signals without applying a gate voltage, which dramatically simplifies the complicated circuit manufacturing process and layout distribution of the sensor. The basic structure of the piezoelectric transistor comprised one or more vertically grown ZnO NWs in contact with the bottom and the top electrodes to form two Schottky contacts. The magnitude and polarity of the piezoelectric potential in a piezoelectric crystal varies with the applied force, which results in the change of the local Schottky barrier height, and then, it directly controls the transmission characteristics of the piezoelectric transistors. Thus, a 2D pressure distribution could be acquired by detecting the current variation of each pixel before and after applying the strain. Nevertheless, the response time (≈0.15 s) of this transistor was larger than the human reaction time. To enhance the response speed of the tactile sensor, Pan et al. developed the first nanowire LED pressure/strain sensor arrays with a response time of 90 ms based on the piezo-phototronic effect, which could directly convert a mechanical stimulation into an optical signal, as shown in Figure 7c.[50] The regular n-ZnO NWs arrays were grown on a p-GaN thin-film substrate along the *c*-axis point to form an array of p–n junction pixel light emitters. Under the compressive strain condition, the piezoelectric polarization charges of NWs were induced to form a local dip in the energy band, which could trap holes near the junctions. This made the carrier injection and recombination rate enhanced, which subsequently leads to a significant increase in the intensity of the emitting light. Hence, the spatial pressure distribution could be observed by using a charge coupled device camera when a convex pattern with the word "PIEZO" was imposed on the device. It should be noted that the intensities of all of the pixels were read out in parallel, leading to the rapid pressure mapping, which provided an effective method for the next generation of TSATMs based on optical communication technology. Furthermore, a flexible ZnO NWs array LED with higher resolution was exhibited by using organic poly (3,4-ethylenedioxythiophene)–polystyrenesulfonic acid films instead of the rigid p-GaN substrate.[51] Similarly, the luminous intensity of each ZnO NW increased linearly with the applied strain to detect and map the trajectory profile spatially.

Recently, tribotronic transistors have also become a research hotspot, in which the frictional electrostatic potential is utilized as a gate signal to regulate the characteristics of the electrical transmission and conversion in semiconductors. TENGs could convert a pressure signal into electricity without applying extra power.[52] The triboelectric potential induced by the coupling effect between contact electrification and electrostatic induction

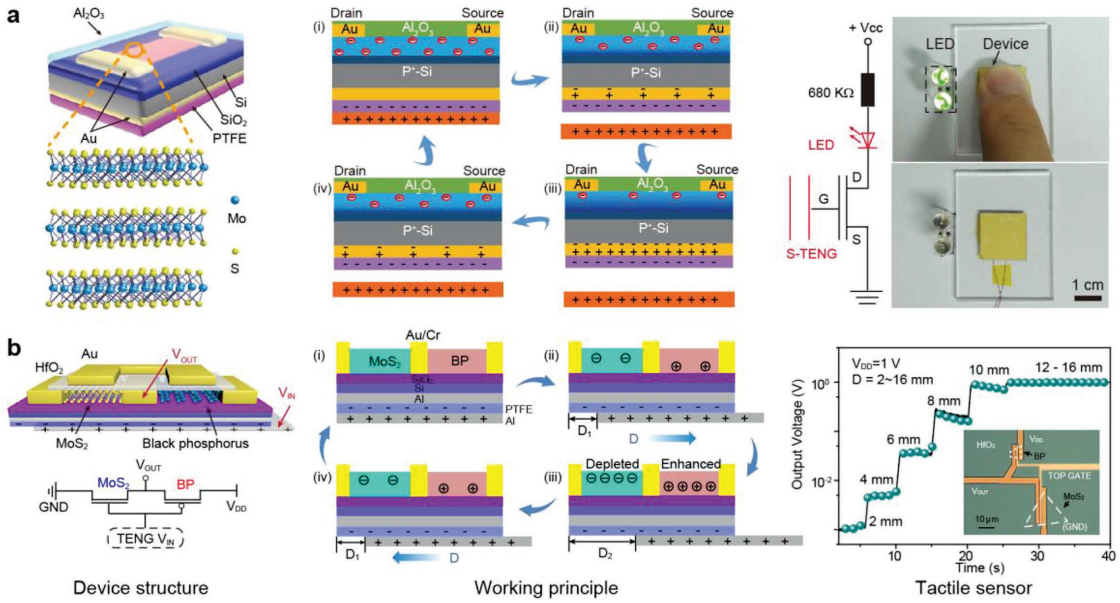

Figure 8. Intrinsic pressure-sensitive transistor based on a novel tribotronic transistor. a) Tactile sensor with MoS_2 tribotronic transistor based on TENG. Reproduced with permission.[55] Copyright 2016, Wiley-VCH Verlag GmbH & Co. KGaA. b) Tunable tribotronic dual-gate logic devices for pressure sensing. Reproduced with permission.[56] Copyright 2018, Wiley-VCH Verlag GmbH & Co. KGaA.

could work as a gate voltage, leading to pressure-dependent tribotronic transistors. Zhang et al. first demonstrated an OTFT combined with a contact-sliding mode TENG, which possessed high transparency, excellent stretchability and stability.[53] Then, they also fabricated a flexible organic triboelectric transistor by using a movable friction layer instead of the top gate electrode, which could generate a drain/source current when it contacted another dielectric layer.[54] This transistor could not only further serve as a pressure sensor with the high sensitivity and fast response time of 110 ms but also be used for the detection of a magnetic field. Furthermore, Xue et al. demonstrated a tribotronic transistor based on the single-electrode mode TENG and molybdenum disulfide FETs with a frictional layer of polytetrafluoroethylene film on the floating gate (**Figure 8**a).[55] The device could detect a tactile signal with the on/off ratio of ≈16, thus providing vivid evidence for the utilization of the tribotronic transistors in human–machine interfaces. Additionally, our group has investigated a tunable tribotronic dual-gate logic device, which has enormous potential for wearable electronics and artificial intelligence (Figure 8b).[56] The effective capacitance increased by adding the high dielectric constant hafnium dioxide (HfO_2) due to the capacitive coupling effect, realizing high-performance, long-term stable, and fast response triboelectric transistors. The work for the first time coupled a dual gate structural logic inverter with a TENG based on n-type Molybdenum disulfide (MoS_2) and p-type black phosphorus, to obtain an active tunable low-power logic device. The electrical characteristics of the device could be controlled by the different frictional displacements of the TENGs, including the modification of the threshold voltage, voltage gain, and static power consumption of the logic inverter. In other words, all of these sensors based on the piezotronic/piezo-phototronic/triboelectric effects were pressure dependent even though no gate electrodes existed in these transistors. This approach provided an opportunity to simplify the fabrication processes and the device structures to achieve a high-resolution, low-power TSATM for applications in wearable devices, health care, and smart manufacturing.

4. Future Trends for the Development of TSATMs

As previously discussed, various types of TSATMs were demonstrated for the large-scale integration of tactile sensors, including the integrated composite structure and the utilization of pressure-dependent transistors.[57] However, there are still challenges, such as novel systems and materials, low-power consumption, and multifunctional design, for practical applications.[58] In this section, we summarize certain recent developments for the TSATM, as follows.

4.1. Novel Systems and Materials

Transistors play a key role in the pressure mapping of large-scale tactile sensors. The transistor should not only possess excellent electrical characteristics but also adapt to various applications, such as stretchability and transparency of the devices. Thus, it is necessary to develop novel systems and materials for the exploration of new trends.[59] Recently, 2D materials, sometimes referred to as single-layer material, possess unusual mechanical and electrical properties for applications in photovoltaics, semiconductors, and electrodes.[60] These can be used as stretchable and transparent channel materials of the transistor or active sensing materials due to their ultrathin structure and pure interface. For example, graphene has been widely used as an active material or channel material for the fabrication of TSATMs.[61] Similarly, molybdenum disulfide

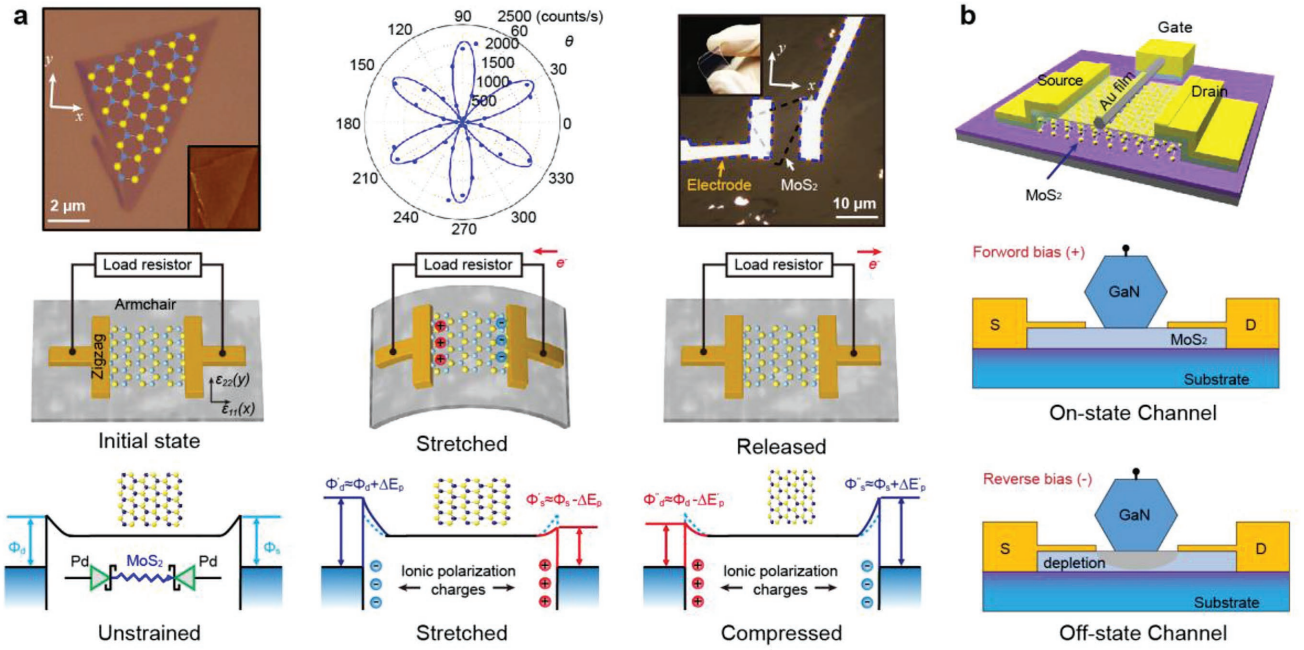

Figure 9. Novel systems and materials in transistors. a) Piezoelectric properties of 2D MoS_2 for promising applications in power storage and stretchable electronics. Reproduced with permission.[63] Copyright 2014, Macmillan Publishers Ltd. b) Self-Aligned MoS_2 FETs with a piezoelectric GaN NW for enhancing the photoresponsivity. Reproduced with permission.[64] Copyright 2016, American Chemical Scoiety.

(MoS_2) possesses superior electrical and optical properties, and it is considered to be a promising alternative material for electronic and optoelectronic sensor devices.[62] Additionally, Wu et al. first observed the piezoelectric properties of MoS_2 experimentally, as shown in **Figure 9**a.[63] They found that the thin MoS_2 flakes would generate the corresponding piezoelectric outputs only in odd-layer MoS_2 rather than in even-layer and bulk crystal. The great potential for applications of MoS_2 was also shown in power supplies, power storage devices and stretchable electronics. Furthermore, we reported a high performance and self-aligned MoS_2 FET based on the piezo-photonic effect with an on–off ratio of $\approx 10^7$ and a subthreshold slope as small as 64 mV dec^{-1} (Figure 9b).[64] The FET consisted of a single layer of MoS_2 and a piezoelectric GaN NW that could enhance the photoresponsivity of the device by the piezo-phototronic effect. Certainly, there are still significant challenges for the tactile detection of these MoS_2 transistors, such as the integrated process of a large-scale matrix and the stretchability of these transistors. However, there is still major motivation and opportunities for the development of 2D materials for fabricating a TSATM with high performance.

4.2. Low-Power Consumption

The energy consumption of a device has long been a common concern for researchers.[65] The utilization of a transistor leads to an energy loss in the process of trajectory scanning due to the requirement of external voltage, even if the researchers prefer a transistor with a lower operating voltage. Thus, is there another way to achieve large-scale trajectory detection with low-power consumption? Recently, various types of tactile sensor matrix were demonstrated based on piezophotonic effect and triboelectric nanogenerators.[66] Our group demonstrated a self-powered pressure sensor matrix based on the mechanoluminescence process that could convert a mechanical stimulation into an optical signal.[67] The core material was ZnS:Mn, whose crystal structure was noncentrosymmetric. Under stain, the energy band structure of ZnS was tilted due to the piezo-photonic effect, which resulted in an increase in the electron–hole recombination. By a nonradioactive recombination, the Mn^{2+} ion excited and then returned to the ground state while visible light was emitting. The device could not only detect the movement trace of a single-point sliding but also map the 2D planar pressure distribution with the assistance of an image acquisition and processing system. It could obtain more personalized information, such as the writing speed and pressure distribution. It became a candidate for next-generation smart sensor networks and human–machine interfaces, to be used in high-level security systems.

Another type of self-power sensor was developed by using TENGs based on the coupling effect between contact electrification and electrostatic induction. Our group demonstrated a large-scale, pressure-sensitive, flexible and durable triboelectric sensor matrix with 16×16 pixels for the dynamic and fast detection of single-point and multipoint touching, as shown in **Figure 10**a.[68] Additionally, a high-resolution cross-type sensor matrix with 32×20 pixels was developed by using cross-locating technology for more rapid tactile mapping and simplification of the device structure, which significantly reduces the addressing lines from $m \times n$ to $m + n$. Compared with the traditional large-scale tactile sensors, the triboelectric sensor matrix exhibited more advantages, such as easy preparation, low cost, and high sensitivity. Furthermore, we reported a highly stretchable and transparent triboelectric tactile sensor by using patterned Ag

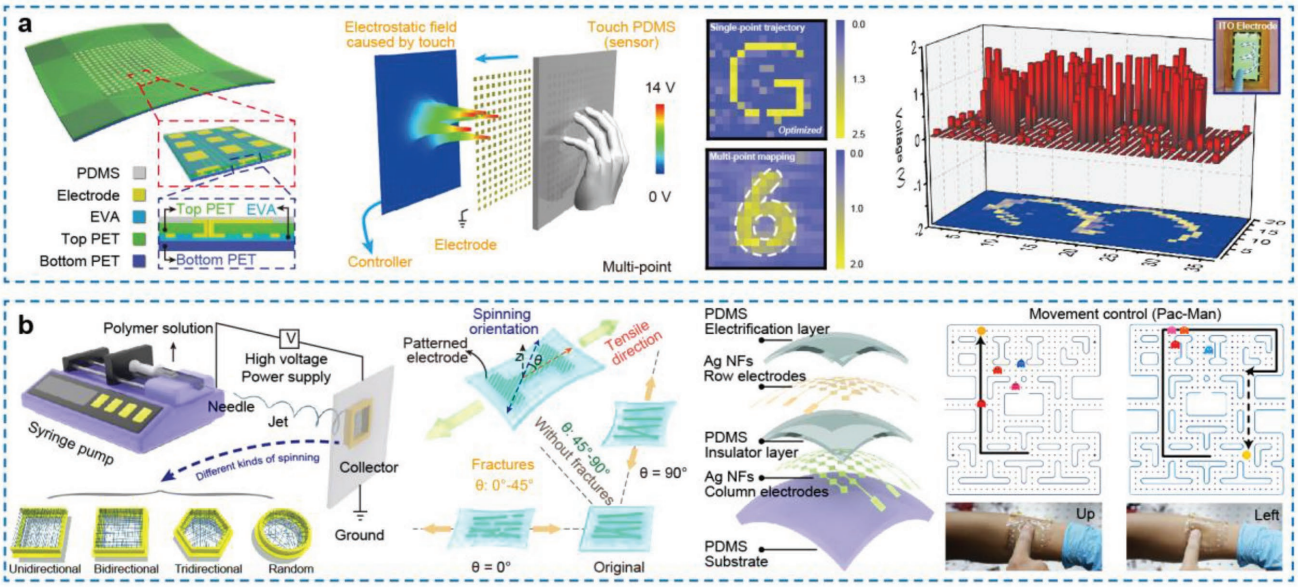

Figure 10. Tactile sensor arrays with low-power consumption based on TENG. a) Self-powered triboelectric tactile sensor matrix for rapid tactile mapping with multiwork modes. Reproduced with permission.[68] Copyright 2016, Wiley-VCH Verlag GmbH & Co. KGaA. b) Highly stretchable and transparent triboelectric tactile sensor matrix based on Ag nanofiber electrodes. Reproduced with permission.[69] Copyright 2018, Wiley-VCH Verlag GmbH & Co. KGaA.

nanofiber electrodes (Figure 10b).[69] Various types of oriented Ag nanofibers were fabricated by electrospinning technology and magnetron sputtering. Patterned Ag nanofiber electrodes that possess low sheet resistance (1.68–11.1 $\Omega\ \square^{-1}$) and high transparency (>70%) can be obtained through the process of photolithography and wet etching. Then, influenced by the effect of electrostatic induction, an 8×8 cross-type triboelectric sensor matrix possessed more excellent stretchable properties. Moreover, real-time tactile mapping can become a possibility due to the optimized structural design and the rapid response time (70 ms). Thus, a powerful platform is provided for artificial electronic skin, smart wearable equipment, and human–machine interactions. In brief, these low-power consumption or self-powered tactile sensors provide novel methods and ideas for the development of TSATMs.

4.3. Multifunctional Design

With the development of critical theories and technologies in Internet of things, it has become a tendency to develop multifunctional electronics for data acquisition and transportation with several sensors, such as different types of strain, temperature, and humidity.[70] Similar to the integrated composite structure of the TSATM, a large-scale multifunctional device can be achieved by assembly with a transistor matrix and a sensing element. Perhaps some other transistors with intrinsic sensing characteristics should be further investigated to realize the measurement of diverse physical parameters. Someya et al. successfully demonstrated a thermally active matrix that consisted of organic transistors and organic diodes.[71] Park et al. exhibited an intrinsic pressure-dependent and temperature-dependent transistor by using piezopyroelectric and piezothermoresistive materials.[72] In addition, Bao and co-workers reported a biocompatibility tactile sensor with repeatable electrically and mechanically self-healing capabilities at room temperature.[73] Their composite material consisted of organic supramolecular polymer and inorganic nanostructured particles, and the remarkable self-healing function was driven by hydrogen bond reassociation between the cut surfaces, which increased the service life of the sensor. Rogers and co-workers first proposed the concept of epidermal electronics, which provided a platform for multifunctional devices.[74] The device possesses outstanding electrical and mechanical performance and can tightly adhere to an irregular plane by van der Waals forces. Recently, we also fabricated stretchable multifunctional integrated sensor arrays that could simultaneously monitor seven physical stimulations, including temperature, humidity, ultraviolet, magnetic, strain, pressure, and proximity stimuli, as shown in **Figure 11**.[75] Based on a polyimide tensile structure network, pluralities of sensors were integrated in 3D stacked structures, and each sensing unit could work independently without any crosstalk. Then, we installed the device on an intelligent prosthesis and found that it could not only provide the tactile function of the prosthesis but also make the prosthesis possess the ability of temperature sensing. In short, the multifunctional design of the device makes it possible to simultaneously monitor diverse physical stimulations in the surroundings, which provides potential applications in human health monitoring and other fields.

5. Conclusions

In this review, we describe the major advances in large-scale TSATMs and their applications in robotics, health care, and

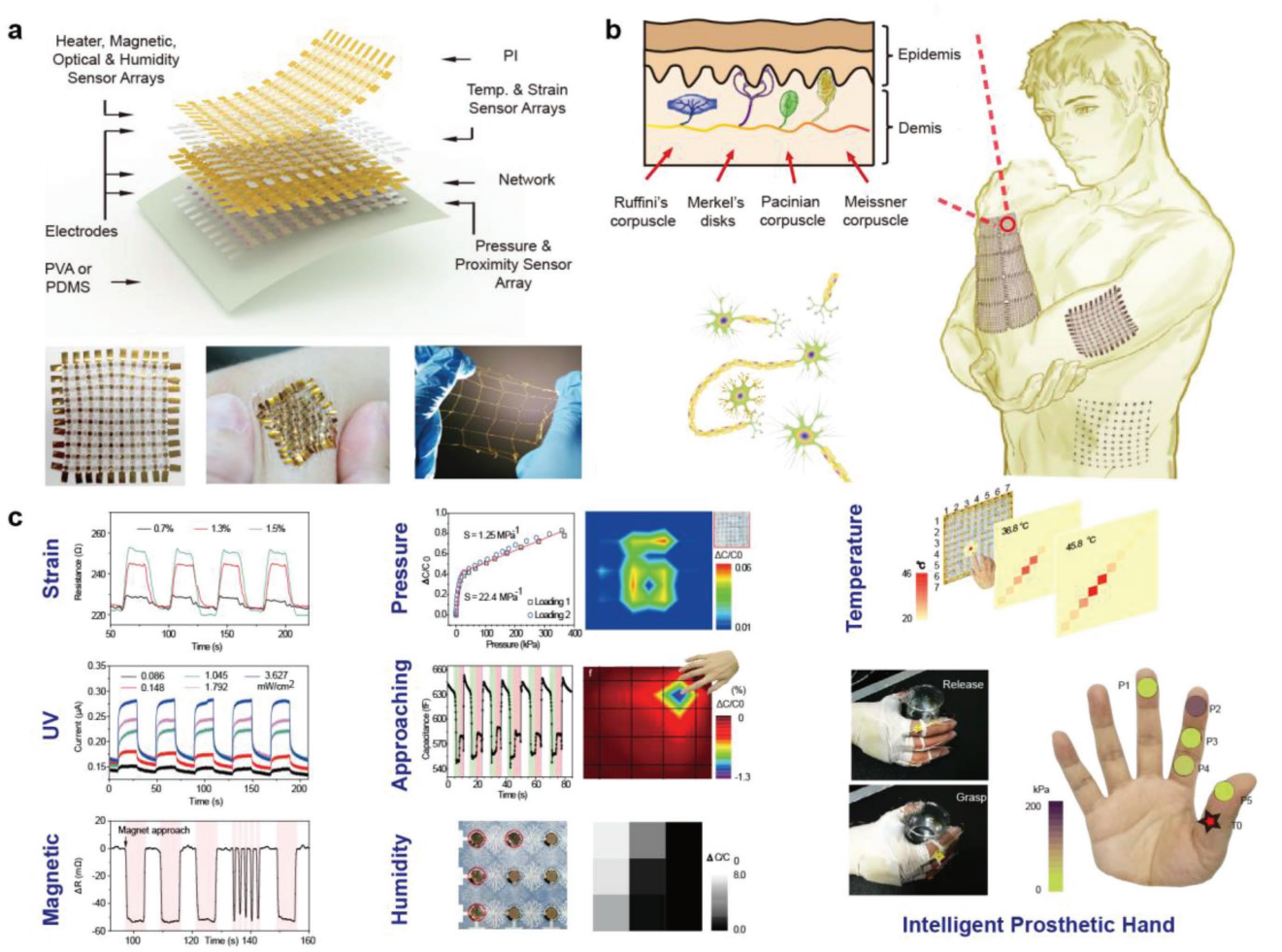

Figure 11. Highly stretchable and conformable matrix network for multifunctional sensing. a) Schematic illustration of an integrated sensor array with seven functions and its objectives. b) Schematic diagram of the device attached to the surface of the human arm and abdomen. c) Multiple physical perceptions and applications in intelligent prosthetic hands, including strain, ultraviolet, magnetic, pressure, approaching, humidity, and temperature. Reproduced with permission.[75] Copyright 2018, Macmillan Publishers Ltd.

smart manufacturing. Recently, tactile sensors based on different transduction methods, including piezoresistivity, capacitance, and piezoelectricity, have been continuously presented. For large-scale pressure mapping, devices composed of transistors have attracted widespread attention, and they reduce the signal crosstalk between each pixel due to their excellent electronic switching capabilities. As is known, the I_D of the transistor has a relationship with the drain/source voltage (V_{DS}), the gate voltage (V_{GS}), and the specific gate capacitance (C_i). Various types of TSATMs were demonstrated by monitoring the change in the I_D of each pixel under strain. First, the integrated composite structure, which consists of a transistor matrix and a pressure-dependent electronic component, was used for the tactile mapping. In this structure, the pressure-dependent materials, including the PSR layer and polymer foils, were integrated between the source electrode of the transistor and the ground acting as the variable source–drain resistance, and the transistor can turn a single-pixel circuit on with a high voltage on its corresponding word line and bit line. Thus, the resistance of the pressure-dependent electronic component changed under the strain, leading to changes in the V_{DS} and I_D. Then, a 2D tactile profile could be obtained by monitoring the I_D of each pixel. Second, various intrinsic pressure-sensitive transistors were exhibited for the simplification of the TSATMs. On the one hand, pressure-dependent transistors based on the change in C_i were demonstrated by using elastic dielectric in the transistor instead of the rigid dielectric. Notably, these devices always possess high pressure sensitivity and a low detection limit of pressure. On the other hand, the pressure-dependent transistors based on the piezotronic effect, piezo-phototronic effect, and triboelectric nanogenerator were further investigated, in which the piezoelectric potential or triboelectric potential could be regarded as a gate voltage. Hence, the TSATM changed from a three-terminal to a two-terminal device, which could be a high-resolution tactile sensor. The rapid development of TSATMs with excellent characteristics over the past few decades will provide a wide range of applications in a variety of industrial fields. Certainly, there are still challenges for practical applications. For example, an advanced manufacturing process, versatile materials, low-power consumption,

and multifunctional design should be explored to meet the needs of various practical applications. It can be foreseen that the TSATM will enhance our quality of life with an improvement in the device performance.

Acknowledgements

Z.H. and Y.P. contributed equally to this work. The authors express thanks for the support from the National Key R&D Project from the Ministry of Science and Technology, China (Grant No. 2016YFA0202703), the National Natural Science Foundation of China (Grant Nos. 51622205, 61675027, 51432005, 61505010, and 51502018), Beijing Council of Science and Technology (Grant Nos. Z171100002017019 and Z181100004418004), the Natural Science Foundation of Beijing Municipality (Grant Nos. 4181004, 4182080, 4184110, and 2184131), and the "Thousand Talents" program of China for pioneering researchers and innovative teams. This article is part of the *Advanced Materials Interfaces* Hall of Fame article series, which highlights the work of top interface and surface scientists.

Conflict of Interest

The authors declare no conflict of interest.

Keywords

electronic skin, large scale, tactile sensor, transistor matrix

Received: July 12, 2018
Revised: August 21, 2018
Published online:

[1] a) T. Q. Trung, N. E. Lee, *Adv. Mater.* **2016**, *28*, 4338; b) X. Wang, L. Dong, H. Zhang, R. Yu, C. Pan, Z. L. Wang, *Adv. Sci.* **2015**, *2*, 1500169; c) M. L. Hammock, A. Chortos, B. C. Tee, J. B. Tok, Z. Bao, *Adv. Mater.* **2013**, *25*, 5997.

[2] a) C. H. Chu, I. Sarangadharan, A. Regmi, Y. W. Chen, C. P. Hsu, W. H. Chang, G. Y. Lee, J. I. Chyi, C. C. Chen, S. C. Shiesh, G. B. Lee, Y. L. Wang, *Sci. Rep.* **2017**, *7*, 15; b) J. Muqiang, X. Kailun, W. Qi, Y. Zhe, W. Huimin, W. Chunya, X. Huanhuan, Z. Mingchao, Z. Yingying, *Adv. Funct. Mater.* **2017**, *27*, 1606066; c) S. Guo, K. Qiu, F. Meng, P. S. Hyun, M. C. McAlpine, *Adv. Mater.* **2017**, *29*, 1701218; d) M. Y. Ma, Z. Zhang, Q. L. Liao, F. Yi, L. H. Han, G. J. Zhang, S. Liu, X. Q. Liao, Y. Zhang, *Nano Energy* **2017**, *32*, 389.

[3] a) C. Dagdeviren, Y. Su, P. Joe, R. Yona, Y. Liu, Y. Kim, Y. Huang, A. R. Damadoran, J. Xia, L. W. Martin, Y. Huang, J. A. Rogers, *Nat. Commun.* **2014**, *5*, 4496; b) L. Pan, C. Alex, G. Yu, Y. Wang, I. Scott, A. Ranulfo, Y. Shi, D. Reinhold, Z. Bao, *Nat. Commun.* **2014**, *5*, 3002.

[4] a) D. Choi, H. Kim, N. Persson, P. Chu, M. Chang, J. Kang, S. Graham, E. Reichmanis, *Chem. Mater.* **2016**, *28*, 1196; b) X. Liu, R. Liang, G. Gao, C. Pan, C. Jiang, Q. Xu, J. Luo, X. Zou, Z. Yang, L. Liao, Z. L. Wang, *Adv. Mater.* **2018**, *30*, 1800932.

[5] a) G. Hu, R. Zhou, R. Yu, L. Dong, C. Pan, Z. L. Wang, *Nano Res.* **2014**, *7*, 1083; b) Z. Chen, Z. Wang, X. Li, Y. Lin, N. Luo, M. Long, N. Zhao, J. Xu, *ACS Nano* **2017**, *11*, 4507.

[6] a) B. Wang, T. Huynh, W. Wu, N. Hayek, T. T. Do, J. C. Cancilla, J. S. Torrecilla, M. M. Nahid, J. M. Colwell, O. M. Gazit, S. R. Puniredd, C. R. McNeill, P. Sonar, H. Haick, *Adv. Mater.* **2016**, *28*, 4012; b) X. Wang, Y. J. Chuan, Y. Longteng, Z. Shuai, L. C. Teck, *Adv. Mater.* **2017**, *2*, 1700016.

[7] J. Bian, N. Wang, J. Ma, Y. Jie, J. Zou, X. Cao, *Nano Energy* **2018**, *47*, 442.

[8] A. Chortos, J. Liu, Z. Bao, *Nat. Mater.* **2016**, *15*, 937.

[9] a) W. Guo, C. Xu, G. Zhu, C. Pan, C. Lin, Z. L. Wang, *Nano Energy* **2012**, *1*, 176; b) B. C. Tee, A. Chortos, A. Berndt, A. K. Nguyen, A. Tom, A. McGuire, Z. C. Lin, K. Tien, W. Bae, H. Wang, P. Mei, H. Chou, B. Cui, K. Deisseroth, T. N. Ng, Z. Bao, *Science* **2015**, *350*, 313; c) R. Bao, C. Wang, Z. Peng, C. Ma, L. Dong, C. Pan, *ACS Photonics* **2017**, *4*, 1344.

[10] a) D. Kim, T. Q. Trung, B. Hwang, J. Kim, S. Jeon, J. Bae, J. Park, N. Lee, *Sci. Rep.* **2015**, *5*, 12705; b) J. Liang, L. Li, D. Chen, H. Tibor, Z. Ren, S. Chou, W. Hu, Q. Pei, *Nat. Commun.* **2015**, *6*, 7647; c) T. Q. Trung, N. T. Tien, D. Kim, M. Jang, O. J. Yoon, N.-E. Lee, *Adv. Funct. Mater.* **2014**, *24*, 117.

[11] a) C. Wan, G. Chen, Y. Fu, M. Wang, N. Matsuhisa, S. Pan, L. Pan, H. Yang, Q. Wan, L. Zhu, X. Chen, *Adv. Mater.* **2018**, *30*, 1801291; b) Y. Kim, A. Chortos, W. Xu, Y. Liu, J. Y. Oh, D. Son, J. Kang, A. M. Foudeh, C. Zhu, Y. Lee, S. Niu, J. Liu, R. Pfattner, Z. Bao, T. W. Lee, *Science* **2018**, *360*, 998.

[12] R. Yu, C. Pan, Y. Hu, L. Li, H. Liu, W. Liu, S. Chua, D. Chi, Z. L. Wang, *Nano Res.* **2013**, *6*, 758.

[13] a) Q. Yang, Y. Liu, C. Pan, J. Chen, X. Wen, Z. L. Wang, *Nano Lett.* **2013**, *13*, 607; b) Z. Wang, R. Yu, X. Wen, Y. Liu, C. Pan, W. Wu, Z. L. Wang, *ACS Nano* **2014**, *8*, 12866; c) S. Qiao, J. H. Liu, G. S. Fu, K. L. Ren, Z. Q. Li, S. F. Wang, C. F. Pan, *Nano Energy* **2018**, *49*, 508; d) C. Pan, S. Niu, Y. Ding, L. Dong, R. Yu, Y. Liu, G. Zhu, Z. L. Wang, *Nano Lett.* **2012**, *12*, 3302; e) G. Hu, W. Guo, R. Yu, X. Yang, R. Zhou, C. Pan, Z. Wang, *Nano Energy* **2016**, *23*, 27; f) X. Li, R. Liang, J. Tao, Z. Peng, Q. Xu, X. Han, X. Wang, C. Wang, J. Zhu, C. Pan, Z. L. Wang, *ACS Nano* **2017**, *11*, 3883.

[14] a) X. Han, W. Du, M. Chen, X. Wang, X. Zhang, X. Li, J. Li, Z. Peng, C. Pan, Z. L. Wang, *Adv. Mater.* **2017**, *29*, 1701253; b) W. Guo, X. Li, M. Chen, L. Xu, L. Dong, X. Cao, W. Tang, J. Zhu, C. Lin, C. Pan, Z. L. Wang, *Adv. Funct. Mater.* **2014**, *24*, 6691; c) X. Yu, X. Han, Z. Zhao, J. Zhang, W. Guo, C. Pan, A. Li, H. Liu, Z. L. Wang, *Nano Energy* **2015**, *11*, 19; d) Q. F. Shi, H. Wang, T. Wang, C. Lee, *Nano Energy* **2016**, *30*, 450; e) T. Chen, M. Zhao, Q. Shi, Z. Yang, H. Liu, L. Sun, J. Ouyang, C. Lee, *Nano Energy* **2018**, *51*, 162; f) H. Askari, Z. Saadatnia, E. Asadi, A. Khajepour, M. B. Khamesee, J. Zu, *Nano Energy* **2018**, *45*, 319.

[15] W. Shockley, *Proc. IRE* **1952**, *40*, 1365.

[16] S. M. Sze, K. K. Ng, *Physics of Semiconductor Devices*, 3rd ed., John Wiley & Sons, New Jersey **2007**.

[17] S. M. Sze, *Semiconductor Devices: Physics and Technology*, 2nd ed., John Wiley & Sons, New York **2002**.

[18] a) M. M. Liu, X. Pu, C. Y. Jiang, T. Liu, X. Huang, L. B. Chen, C. H. Du, J. M. Sun, W. G. Hu, Z. L. Wang, *Adv. Mater.* **2017**, *29*, 1703700; b) X. Wang, M. Que, M. Chen, X. Han, X. Li, C. Pan, Z. L. Wang, *Adv. Mater.* **2017**, *29*, 1605817.

[19] a) Y. Zang, H. Shen, D. Huang, C. Di, D. Zhu, *Adv. Mater.* **2017**, *29*, 1606088; b) F. A. Viola, A. Spanu, P. C. Ricci, A. Bonfiglio, P. Cosseddu, *Sci. Rep.* **2018**, *8*, 8073.

[20] a) C. Yeom, K. Chen, D. Kiriya, Z. Yu, G. Cho, A. Javey, *Adv. Mater.* **2015**, *27*, 1561; b) Y. Gao, H. Ota, E. W. Schaler, K. Chen, A. Zhao, W. Gao, H. M. Fahad, Y. Leng, A. Zheng, F. Xiong, C. Zhang, L. C. Tai, P. Zhao, R. S. Fearing, A. Javey, *Adv. Mater.* **2017**, *29*, 1701985; c) L. Xiang, H. Zhang, G. Dong, D. Zhong, J. Han, X. Liang, Z. Zhang, L. M. Peng, Y. Hu, *Nat. Electron.* **2018**, *1*, 237.

[21] T. Someya, T. Sekitani, S. Iba, Y. Kato, H. Kawaguchi, T. Sakurai, *Proc. Natl. Acad. Sci. USA* **2004**, *101*, 9966.

[22] a) G. Yu, J. Hu, J. Tan, Y. Gao, Y. Lu, F. Xuan, *Nanotechnology* **2018**, *29*, 115502; b) Q. Wang, M. Jian, C. Wang, Y. Zhang, *Adv. Funct. Mater.* **2017**, *27*, 1605657.

[23] M. Kaltenbrunner, T. Sekitani, J. Reeder, T. Yokota, K. Kuribara, T. Tokuhara, M. Drack, R. Schwodiauer, I. Graz, S. BauerGogonea, S. Bauer, T. Someya, *Nature* **2013**, *499*, 458.

[24] C. Wang, D. Hwang, Z. Yu, K. Takei, J. Park, T. Chen, B. Ma, A. Javey, *Nat. Mater.* **2013**, *12*, 899.
[25] T. Sekitani, T. Yokota, U. Zschieschang, H. Klauk, S. Bauer, K. Takeuchi, M. Takamiya, T. Sakurai, T. Someya, *Science* **2009**, *326*, 1516.
[26] L. Nela, J. Tang, Q. Cao, G. Tulevski, S. Han, *Nano Lett.* **2018**, *18*, 2054.
[27] K. Takei, T. Takahashi, J. C. Ho, H. Ko, A. G. Gillies, P. W. Leu, R. S. Fearing, A. Javey, *Nat. Mater.* **2010**, *9*, 821.
[28] a) A. Chortos, G. I. Koleilat, R. Pfattner, D. Kong, P. Lin, R. Nur, T. Lei, H. Wang, N. Liu, Y. C. Lai, *Adv. Mater.* **2016**, *28*, 4441; b) C. Kevin, G. Wei, E. Sam, K. Daisuke, O. Hiroki, N. H. Y. Yin, T. Kuniharu, J. Ali, *Adv. Mater.* **2016**, *28*, 4397.
[29] T. Takahashi, K. Takei, A. G. Gillies, R. S. Fearing, A. Javey, *Nano Lett.* **2011**, *11*, 5408.
[30] M. Shin, J. H. Song, G. H. Lim, B. Lim, J. J. Park, U. Jeong, *Adv. Mater.* **2014**, *26*, 3706.
[31] T. Sekitani, Y. Noguchi, K. Hata, T. Fukushima, T. Aida, T. Someya, *Science* **2008**, *321*, 1468.
[32] S. Y. Hong, Y. H. Lee, H. Park, S. W. Jin, Y. R. Jeong, J. Yun, I. You, G. Zi, J. S. Ha, *Adv. Mater.* **2016**, *28*, 930.
[33] A. Chortos, J. Lim, J. W. To, M. Vosgueritchian, T. J. Dusseault, T. H. Kim, S. Hwang, Z. Bao, *Adv. Mater.* **2014**, *26*, 4253.
[34] J. Y. Oh, S. RondeauGagne, Y. C. Chiu, A. Chortos, F. Lissel, G. N. Wang, B. C. Schroeder, T. Kurosawa, J. Lopez, T. Katsumata, J. Xu, C. Zhu, X. Gu, W. G. Bae, Y. Kim, L. Jin, J. W. Chung, J. B. Tok, Z. Bao, *Nature* **2016**, *539*, 411.
[35] J. Xu, S. Wang, G. N. Wang, C. Zhu, S. Luo, L. Jin, X. Gu, S. Chen, V. R. Feig, J. W. F. To, S. Rondeau-Gagné, J. Park, B. C. Schroeder, C. Lu, J. Y. Oh, Y. Wang, Y. Kim, H. Yan, R. Sinclair, D. Zhou, G. Xue, B. Murmann, C. Linder, W. Cai, J. B. H. Tok, J. W. Chung, Z. Bao, *Science* **2017**, *355*, 59.
[36] S. Wang, J. Xu, W. Wang, G. N. Wang, R. Rastak, F. Molina-Lopez, J. W. Chung, S. Niu, V. Feig, J. Lopez, T. Lei, S.-K. Kwon, Yeongin, A. M. Foudeh, A. Ehrlich, A. Gasperini, Y. Yun, B. Murmann, J. B. Tok, Z. Bao, *Nature* **2018**, *555*, 83.
[37] a) D. Kong, R. Pfattner, A. Chortos, C. Lu, A. C. Hinckley, C. Wang, W.-Y. Lee, J. W. Chung, Z. Bao, *Adv. Funct. Mater.* **2016**, *26*, 4680; b) A. Kyaw, H. Loh, F. Yan, J. Xu, *J. Mater. Chem. C* **2017**, *5*, 12039.
[38] S. C. Mannsfeld, B. C. Tee, R. M. Stoltenberg, C. V. Chen, S. Barman, B. V. Muir, A. N. Sokolov, C. Reese, Z. Bao, *Nat. Mater.* **2010**, *9*, 859.
[39] S. Choi, H. Lee, R. Ghaffari, T. Hyeon, D. H. Kim, *Adv. Mater.* **2016**, *28*, 4203.
[40] G. Schwartz, B. C. K. Tee, J. Mei, A. L. Appleton, D. H. Kim, H. Wang, Z. Bao, *Nat. Commun.* **2013**, *4*, 1859.
[41] L. Viry, A. Levi, M. Totaro, A. Mondini, V. Mattoli, B. Mazzolai, L. Beccai, *Adv. Mater.* **2014**, *26*, 2659.
[42] Y. Zang, F. Zhang, D. Huang, X. Gao, C. Di, D. Zhu, *Nat. Commun.* **2015**, *6*, 6269.
[43] S. H. Shin, S. Ji, S. Choi, K. H. Pyo, B. W. An, J. Park, J. Kim, J. Y. Kim, K. S. Lee, S. Y. Kwon, J. Heo, B. G. Park, J. U. Park, *Nat. Commun.* **2017**, *8*, 14950.
[44] S. Liu, L. Wang, X. Feng, Z. Wang, Q. Xu, S. Bai, Y. Qin, Z. L. Wang, *Adv. Mater.* **2017**, *29*, 1606346.
[45] a) H. Zeng, G. Duan, Y. Li, S. Yang, X. Xu, W. Cai, *Adv. Funct. Mater.* **2010**, *20*, 561; b) S. Stassi, V. Cauda, C. Ottone, A. Chiodoni, C. F. Pirri, G. Canavese, *Nano Energy* **2015**, *13*, 474; c) C. F. Wang, R. R. Bao, K. Zhao, T. P. Zhang, L. Dong, C. F. Pan, *Nano Energy* **2015**, *14*, 364; d) R. Zhou, G. Hu, R. Yu, C. Pan, Z. L. Wang, *Nano Energy* **2015**, *12*, 588; e) R. Yu, C. Pan, J. Chen, G. Zhu, Z. L. Wang, *Adv. Funct. Mater.* **2013**, *23*, 5868; f) R. Yu, C. Pan, Z. L. Wang, *Energy Environ. Sci.* **2013**, *6*, 494.
[46] a) R. Yu, L. Dong, C. Pan, S. Niu, H. Liu, W. Liu, S. Chua, D. Chi, Z. L. Wang, *Adv. Mater.* **2012**, *24*, 3532; b) F. Xue, L. J. Yang, M. X. Chen, J. Chen, X. N. Yang, L. F. Wang, L. B. Chen, C. F. Pan, Z. L. Wang, *NPG Asia Mater.* **2017**, *9*, 6.
[47] a) Y. Zhou, K. Wang, W. Han, S. Rai, Y. Zhang, Y. Ding, C. Pan, F. Zhang, W. Zhou, Z. L. Wang, *ACS Nano* **2012**, *6*, 6478; b) L. Dong, S. Niu, C. Pan, R. Yu, Y. Zhang, Z. L. Wang, *Adv. Mater.* **2012**, *24*, 5470; c) R. Bao, C. Wang, D. Lin, C. Shen, K. Zhao, C. Pan, *Nanoscale* **2016**, *8*, 8078; d) L. Zhu, L. Wang, F. Xue, L. Chen, J. Fu, X. Feng, T. Li, Z. Wang, *Adv. Sci.* **2017**, *4*, 1600185.
[48] a) M. Chen, B. Zhao, G. Hu, X. Fang, H. Wang, L. Wang, J. Luo, X. Han, X. Wang, C. Pan, Z. L. Wang, *Adv. Funct. Mater.* **2018**, *28*, 1706379; b) S. Qiao, J. Liu, X. Niu, B. Liang, G. Fu, Z. Li, S. Wang, K. Ren, C. Pan, *Adv. Funct. Mater.* **2018**, *28*, 1707311.
[49] W. Wu, X. Wen, Z. Wang, *Science* **2013**, *340*, 952.
[50] C. Pan, L. Dong, G. Zhu, S. Niu, R. Yu, Q. Yang, Y. Liu, Z. L. Wang, *Nat. Photonics* **2013**, *7*, 752.
[51] R. Bao, C. Wang, L. Dong, R. Yu, K. Zhao, Z. L. Wang, C. Pan, *Adv. Funct. Mater.* **2015**, *25*, 2884.
[52] a) T. Li, J. Zou, F. Xing, M. Zhang, X. Cao, N. Wang, Z. L. Wang, *ACS Nano* **2017**, *11*, 3950; b) X. Pu, M. Liu, X. Chen, J. Sun, C. Du, Y. Zhang, J. Zhai, W. Hu, Z. L. Wang, *Sci. Adv.* **2017**, *3*, 1700015; c) Z. Yuan, T. Zhou, Y. Yin, R. Cao, C. Li, Z. Wang, *ACS Nano* **2017**, *11*, 8364.
[53] C. Zhang, Z. Zhang, X. Yang, T. Zhou, C. B. Han, Z. Wang, *Adv. Funct. Mater.* **2016**, *26*, 2554.
[54] J. Zhao, H. Guo, Y. Pang, F. Xi, Z. Yang, G. Liu, T. Guo, G. Dong, C. Zhang, Z. Wang, *ACS Nano* **2017**, *11*, 11566.
[55] F. Xue, L. Chen, L. Wang, Y. Pang, J. Chen, C. Zhang, Z. L. Wang, *Adv. Funct. Mater.* **2016**, *26*, 2104.
[56] G. Gao, B. Wan, X. Liu, Q. Sun, X. Yang, L. Wang, C. Pan, Z. L. Wang, *Adv. Mater.* **2018**, *30*, 1705088.
[57] J. K. Song, D. Son, J. Kim, Y. J. Yoo, G. J. Lee, L. Wang, M. K. Choi, J. Yang, M. Lee, K. Do, J. H. Koo, N. S. Lu, J. H. Kim, T. Hyeon, Y. M. Song, D. H. Kim, *Adv. Funct. Mater.* **2017**, *27*, 9.
[58] a) F. J. Berger, T. M. Higgins, M. Rother, A. Graf, Y. Zakharko, S. Allard, M. Matthiesen, J. M. Gotthardt, U. Scherf, J. Zaumseil, *ACS Appl. Mater. Interfaces* **2018**, *10*, 11135; b) C. Wan, G. Chen, Y. Fu, M. Wang, N. Matsuhisa, S. Pan, L. Pan, H. Yang, Q. Wan, L. Zhu, X. Chen, *Adv. Mater.* **2018**, *0*, 1801291.
[59] a) Y. Pang, K. Zhang, Z. Yang, S. Jiang, Z. Ju, Y. Li, X. Wang, D. Wang, M. Jian, Y. Zhang, R. Liang, H. Tian, Y. Yang, T. Ren, *ACS Nano* **2018**, *12*, 2346; b) M. Xu, J. Qi, F. Li, X. Liao, S. Liu, Y. Zhang, *RSC Adv.* **2017**, *7*, 30506.
[60] a) M. Kang, J. Kim, B. Jang, Y. Chae, J. Kim, J.-H. Ahn, *ACS Nano* **2017**, *11*, 7950; b) S. Goossens, G. Navickaite, C. Monasterio, S. Gupta, J. J. Piqueras, R. Pérez, G. Burwell, I. Nikitskiy, T. Lasanta, T. Galán, E. Puma, A. Centeno, A. Pesquera, A. Zurutuza, G. Konstantatos, F. Koppens, *Nat. Photonics* **2017**, *11*, 366.
[61] a) S. Lee, B. J. Kim, H. Jang, S. C. Yoon, C. Lee, B. H. Hong, J. A. Rogers, J. H. Cho, J. Ahn, *Nano Lett.* **2011**, *11*, 4642; b) B. Zhu, Z. Niu, H. Wang, W. R. Leow, H. Wang, Y. Li, L. Zheng, J. Wei, F. Huo, X. Chen, *Small* **2014**, *10*, 3625; c) T. T. Quang, T. N. Thanh, K. Doil, J. Mi, Y. O. Ja, L. Nae-Eung, *Adv. Funct. Mater.* **2014**, *24*, 117.
[62] a) W. Wu, L. Wang, R. Yu, Y. Liu, S. H. Wei, J. Hone, Z. L. Wang, *Adv. Mater.* **2016**, *28*, 8463; b) P. Minhoon, P. Y. Ju, C. Xiang, P. Yon-Kyu, K. Min-Seok, A. Jong-Hyun, *Adv. Mater.* **2016**, *28*, 2556; c) J. Zhao, N. Li, H. Yu, Z. Wei, M. Liao, P. Chen, S. Wang, D. Shi, Q. Sun, G. Zhang, *Adv. Mater.* **2017**, *29*, 1702076; d) A. Nourbakhsh, A. Zubair, S. Joglekar, M. Dresselhaus, T. Palacios, *Nanoscale* **2017**, *9*, 6122.
[63] W. Wu, L. Wang, Y. Li, F. Zhang, L. Lin, S. Niu, D. Chenet, X. Zhang, Y. Hao, T. F. Heinz, J. Hone, Z. L. Wang, *Nature* **2014**, *514*, 470.
[64] X. Liu, X. Yang, G. Gao, Z. Yang, H. Liu, Q. Li, Z. Lou, G. Shen, L. Liao, C. Pan, Z. L. Wang, *ACS Nano* **2016**, *10*, 7451.
[65] a) K. Kim, M. Jung, B. Kim, J. Kim, K. Shin, O. S. Kwon, S. Jeon, *Nano Energy* **2017**, *41*, 301; b) L. Jin, J. Tao, R. Bao, L. Sun, C. Pan, *Sci. Rep.* **2017**, *7*, 10521; c) S. Rohit, P. Long, M. Vivek, *Adv. Mater.*

2018, *30*, 1705778; d) T. Bu, T. Xiao, Z. Yang, G. Liu, X. Fu, J. Nie, T. Guo, Y. Pang, J. Zhao, F. Xi, C. Zhang, Z. L. Wang, *Adv. Mater.* **2018**, *30*, 1800066; e) Q. Zhang, T. Jiang, D. Ho, S. Qin, X. Yang, J. H. Cho, Q. Sun, Z. L. Wang, *ACS Nano* **2018**, *12*, 254.

[66] a) H. X. He, Y. M. Fu, W. L. Zang, Q. Wang, L. L. Xing, Y. Zhang, X. Y. Xue, *Nano Energy* **2017**, *31*, 37; b) F. B. Xi, Y. K. Pang, W. Li, T. Jiang, L. M. Zhang, T. Guo, G. X. Liu, C. Zhang, Z. L. Wang, *Nano Energy* **2017**, *37*, 168; c) M. F. Lin, J. Q. Xiong, J. X. Wang, K. Parida, P. S. Lee, *Nano Energy* **2018**, *44*, 248.

[67] X. Wang, H. Zhang, R. Yu, L. Dong, D. Peng, A. Zhang, Y. Zhang, H. Liu, C. Pan, Z. L. Wang, *Adv. Mater.* **2015**, *27*, 2324.

[68] X. Wang, H. Zhang, L. Dong, X. Han, W. Du, J. Zhai, C. Pan, Z. L. Wang, *Adv. Mater.* **2016**, *28*, 2896.

[69] X. Wang, Y. Zhang, X. Zhang, Z. Huo, X. Li, M. Que, Z. Peng, H. Wang, C. Pan, *Adv. Mater.* **2018**, *30*, 1706738.

[70] a) X. Ren, K. Pei, B. Peng, Z. Zhang, Z. Wang, X. Wang, P. K. L. Chan, *Adv. Mater.* **2016**, *28*, 4832; b) I. Graz, M. Krause, S. Bauer-Gogonea, S. Bauer, S. P. Lacour, B. Ploss, M. Zirkl, B. Stadlober, S. Wagner, *J. Appl. Phys.* **2009**, *106*, 034503.

[71] T. Someya, Y. Kato, T. Sekitani, S. Iba, Y. Noguchi, Y. Murase, H. Kawaguchi, T. Sakurai, *Proc. Natl. Acad. Sci. USA* **2005**, *102*, 12321.

[72] N. T. Tien, S. Jeon, D. Kim, T. Q. Trung, M. Jang, B. Hwang, K. Byun, J. Bae, E. Lee, J. B. Tok, Z. Bao, N. Lee, J. Park, *Adv. Mater.* **2014**, *26*, 796.

[73] B. C. K. Tee, C. Wang, R. Allen, Z. Bao, *Nat. Nanotechnol.* **2012**, *7*, 825.

[74] D. Kim, N. Lu, R. Ma, Y. Kim, R. Kim, S. Wang, J. Wu, S. M. Won, H. Tao, A. Islam, K. J. Yu, T. Kim, R. Chowdhury, M. Ying, L. Xu, M. Li, H. Chung, H. Keum, M. McCormick, P. Liu, Y. Zhang, F. G. Omenetto, Y. Huang, T. Coleman, J. A. Rogers, *Science* **2011**, *333*, 838.

[75] Q. Hua, J. Sun, H. Liu, R. Bao, R. Yu, J. Zhai, C. Pan, Z. L. Wang, *Nat. Commun.* **2018**, *9*, 244.

